Longitudinal In Vivo imaging of ¹²⁵I-Labeled Gold Nanoparticles using Multi-Pinhole X-Ray Fluorescence Imaging System

Taeyun Kim a, Hwijoon Jeong a, Taewan Kim A, Sung-Joon Ye a,b,c,d*

^aDepartment of Applied Bioengineering, Graduate School of Convergence Science and Technology, Seoul National University, Seoul, 08826, Republic of Korea

^bResearch Institute for Convergence Science, Seoul National University, Seoul, 08826, Republic of Korea ^cAdvanced Institute of Convergence Technology, Seoul National University, Suwon, 16229, Republic of Korea ^dT-ROH Inc., Seoul, 08813, Republic of Korea

*Corresponding author: sye@snu.ac.kr

1. Introduction

Metal nanoparticles (MNPs) are in demand as drug delivery materials and radiosensitizers due to their unique physical and chemical properties [1]. Compared to other high atomic number materials, such as gadolinium, platinum, silver, and hafnium, gold nanoparticles (GNPs) are particularly promising because they are inert metals that exhibit excellent biocompatibility and low toxicity [2, 3]. They can be precisely controlled in terms of size and shape to match the microenvironment of the targeted tumor, and their surface can be modified to enhance their targeting ability. For preclinical and clinical applications, a quantitative imaging modality is required for determining the in vivo biodistribution of GNPs.

X-ray fluorescence (XRF) imaging is a technique that measures XRF photons emitted from a target material. Using the XRF photons generated through the interaction between GNP and labeled medical radioisotopes, such as ¹²⁵I, ¹⁶⁶Ho, and ¹⁷⁷Lu, is a promising approach for effective clinical treatment applications [4, 5]. An XRF imaging system, which uses GNPs as a contrast agent, is configured as a benchtop setup and enables the evaluation of biodistribution and the quantitative analysis of GNP concentration.

In this study, CT-26 tumor-bearing BALB/c mice were injected with ¹²⁵I-labeled GNP solutions at different radioactivity. A calibration curve for the correlation between radioactivity and photon counts was acquired using a multi-pinhole XRF imaging system. The residual radioactivity was quantitatively evaluated according to the injection time based on the obtained calibration curve. These results demonstrate the validity and feasibility of using the XRF imaging system to evaluate the in vivo biodistribution and quantification of ¹²⁵I-labeled GNP.

2. Materials and Methods

XRF photons passed through a tungsten multi-pinhole collimator (four pinholes, 2 mm inner diameter) and are recorded with a 160 \times 160-pixel cadmium telluride (CdTe) detector with pixel pitch of 250 μm . The object-to-collimator and collimator-to-detector distances were set to 15 cm and 5 cm, respectively, yielding $3\times$ minification.

A solution of $^{125}\text{I-labeled}$ GNP was prepared using two BALB/c mice bearing CT-26 tumor. To acquire a correlation between radioactivity and photon counts, the initial radioactivity of the injected solution was set to 3.9, 7.8, 15.6, 31.3, 62.5, 125, 250, 500, and 1,000 $\mu\text{Ci. XRF}$ images were then acquired under each condition with a scan time of 10 minutes. Then, the quantitative correlation between radioactivity and photon counts was evaluated.

After evaluating the calibration curve, intratumoral injection of 500 μ Ci of the 125 I-labeled GNP solution was conducted, and XRF images were acquired at 0, 3, 24, 48, 72, and 96 hours. The calibration curve was then used to quantify residual radioactivity in the tumor over time.

3. Result and Discussion

Fig. 1 shows multi-pinhole XRF images corresponding to different levels of radioactivity. A multi-pinhole collimator generated four pinhole projections. Even under the lowest radioactivity condition of 3.9 μ Ci, clear images could be obtained, confirming the performance of this XRF imaging system.

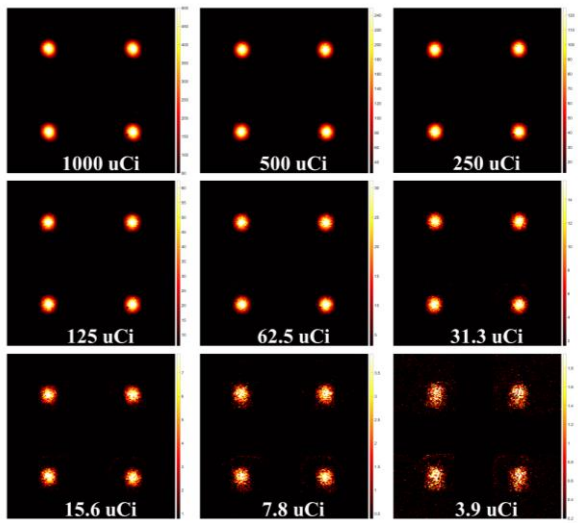


Fig. 1. Multi-pinhole XRF images of a ¹²⁵I-labeled GNP with different radioactivity.

Fig. 2 shows the calibration curve indicating the quantitative relationship between photon counts and radioactivity, measured using 125 I-labeled GNP solutions having different radioactivity. The photon counts corresponding to each radioactivity showed good linearity ($R^2 = 0.998$), enabling the quantification of radioactivity according to photon counts.

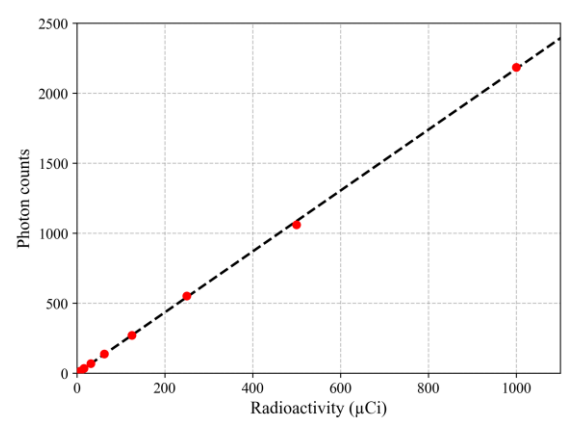


Fig. 2. Calibration curve of radioactivity and photon counts.

Fig. 3 shows the excretion curve of radioactivity in the tumor over time after 500 μ Ci solution injection. After reaching a maximum immediately after injection, the radioactivity decreases continuously over time due to the effects of metabolism and excretion processes in the body. This curve was obtained by applying the previously acquired calibration curve to convert the XRF photon counts at each time point into radioactivity, demonstrating that the residual amount of ¹²⁵I-labeled GNP can be evaluated and quantified.

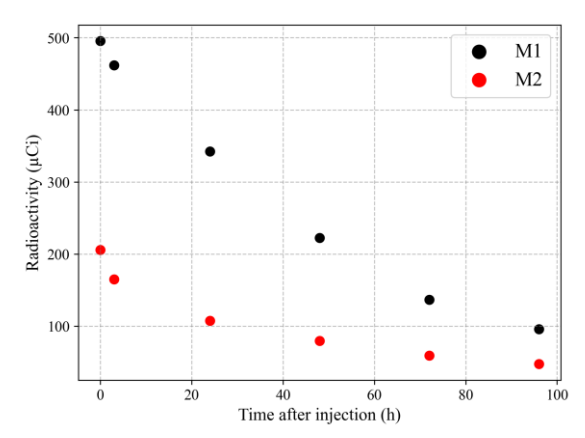


Fig. 3. Excretion curve of radioactivity in the body after the injection.

4. Conclusion

This study demonstrated that imaging and quantitative analysis of $^{125}\text{I-labeled}$ GNP is applicable using the XRF imaging system. Imaging the signal at a low radioactivity of 3.9 μCi showed the good performance of the proposed measurement configuration. The calibration curve was

acquired under different initial radioactivity conditions, and these were applied to quantitatively evaluate the residual radioactivity in the tumor over time after intratumoral injection. The limitations of this study include the small number of subjects (n=2) and a measurement condition (e.g., short scan time, single measurement). In further studies, it is necessary to improve the measurement condition and cross-validation with other quantitative analysis methods, such as inductively coupled plasma mass spectrometry. Additionally, adding computed tomography to the system will not only overcome the functional information from the XRF imaging system but also provide anatomical information [6]. Overall, this study demonstrated the feasibility of the evaluation and quantification of 125I-labeled GNP using the XRF imaging system.

Acknowledgements

This work was supported by a National Research Foundation of Korea (NRF) grant funded by the Korea government (MSIT) (RS-2023-00237149) and by Basic Science Research Program through the National Research Foundation of Korea (NRF) funded by the Ministry of Education (2022R1A6A1A03063039).

REFERENCES

- [1] T. Kim, R. Hernández Millares, T. Kim, M. Eom, J. Kim, and S.J. Ye, Nanoscale dosimetry for a radioisotope-labeled metal nanoparticle using MCNP6.2 and Geant4, Med. Phys., Vol. 51, p. 9290–9302, 2024.
- [2] T. Kim, W. Lee, M. Jeon, H. Kim, M. Eom, S. Jung, H.J. Im, and S.J. Ye, Dual imaging modality of fluorescence and transmission X-rays for gold nanoparticle-injected living mice, Med. Phys., Vol. 50, p. 529–539, 2023.
- [3] S. Jung, T. Kim, W. Lee, H. Kim, H.S. Kim, H.J. Im, and S.J. Ye, Dynamic in vivo X-ray fluorescence imaging of gold in living mice exposed to gold nanoparticles, IEEE Trans. Med. Imaging., Vol. 39, p. 526–533, 2019.
- [4] T. Kim, B.Y. Han, S. Yang, J. Lee, G.M. Sun, B.G. Park, and S.J. Ye, Thermal-hydraulic safety analysis of radioisotope production in HANARO using MCNP6 and COMSOL multiphysics: A feasibility study, Nucl. Eng. Technol., Vol. 55, p. 3996–4001, 2023.X
- [5] T. Kim, B.Y. Han, S. Yang, J. Lee, G.M. Sun, B.G. Park, and S.J. Ye, Systematic analysis for the thermal stability assessment of ¹⁶⁶Ho production using HANARO: An in silico study, Nucl. Eng. Technol., Vol. 56, p. 4914–4920, 2024.
- [6] T. Kim, J. Lee, G.M. Sun, B.G. Park, H.J. Park, D.S. Choi, and S.J. Ye, Comparison of X-ray computed tomography and magnetic resonance imaging to detect pest-infested fruits: A pilot study, Nucl. Eng. Technol., Vol. 54, p. 514–522, 2022.